PROGRESS IN ENGINEERING APPLICATION AND TECHNOLOGY
e-ISSN: 2773-5303

PEAT

Vol. 6 No. 1 (2025) p. 41-50
https://publisher.uthm.edu.my/periodicals/index.php/peat

Removal of Methyl Orange using Nanofibrillated Cellulose (NFC) from Kenaf via Cross-Flow Filtration System

Batrisyia Aina Kamaruzaini[1], Nor Hazren Abdul Hamid[1]*, Nur Hanis Hayati Hairom[1], Mohamad Zayani Zakwan Mohd Zin[2]

[1] *Department of Civil Engineering Technology, Faculty of Engineering Technology Universiti Tun Hussein Onn Malaysia, 86400, Pagoh, Johor, MALAYSIA*
[2] *Cluster of Civil and Chemical Engineering Technology, Laboratory Management Office Universiti Tun Hussein Onn Malaysia, 86400, Pagoh, Johor, MALAYSIA*

*Corresponding Author: norhazren@uthm.edu.my
DOI: https://doi.org/10.30880/peat.2025.06.01.005

Article Info

Received: 19 January 2025
Accepted: 06 February 2025
Available online: 30 April 2025

Keywords

Methyl orange, Dye wastewater, Nanofibrillated cellulose, Response Surface Methodology, Fouling mechanism

Abstract

The increasing presence of synthetic dyes in textile wastewater poses a significant environmental challenge, requiring sustainable and efficient filtration technologies. This study explores the application of nanofibrillated cellulose (NFC) filter paper derived from Kenaf fibers to remove Methyl Orange (MO) dye in a cross-flow filtration system. Response Surface Methodology (RSM) with Central Composite Design (CCD) was applied to optimise key parameters, including pH, dye concentration, and pressure, to maximise dye removal efficiency and normalised flux performance. The optimal conditions at pH 10, 1000 ADMI dye concentration, and 3 bar pressure achieved a maximum dye removal efficiency of 54.74 % and a normalised flux of 0.5436. The fouling analysis confirmed cake layer formation as the dominant mechanism, leading to a gradual decline in flux, which was further validated using FESEM and AFM analyses, revealing significant structural modifications in the NFC filter paper post-filtration. The observed morphological changes, including increased fiber compaction and surface roughness reduction, indicate fouling-induced performance limitations, highlighting the necessity for anti-fouling strategies to maintain long-term filtration efficiency. Despite its promising performance in dye removal, the treated wastewater did not fully meet regulatory discharge limits, suggesting additional treatment processes are needed to enhance water quality compliance.

1. Introduction

The rapid industrialisation and expansion of manufacturing activities have significantly contributed to environmental pollution, mainly by discharging untreated wastewater into natural water bodies. Among various industrial sectors, the textile industry is a major contributor to global water contamination due to the extensive use of synthetic dyes. These dyes, particularly azo dyes such as methyl orange (MO), exhibit high stability, toxicity, and resistance to biodegradation, making their removal from wastewater a pressing environmental challenge [1]. In Malaysia, the textile industry accounts for a significant proportion of industrial wastewater discharge, with substantial amounts of dye pollutants entering water bodies [2,3]. The persistence of MO in wastewater significantly reduces water transparency, impairs photosynthetic activity in aquatic plants, and introduces severe carcinogenic and mutagenic risks to human and ecosystem health [4]. These issues

underscore the necessity of developing sustainable, efficient, and cost-effective wastewater treatment technologies.

Numerous wastewater treatment methods have been explored to mitigate dye pollution, including chemical coagulation, biological treatment, oxidation, adsorption, and membrane filtration [5]. Although chemical and biological processes have been widely employed, they often face limitations such as high operational costs, secondary pollution, and incomplete dye degradation [6]. Membrane-based filtration, particularly nanofiltration (NF) and cross-flow filtration systems has demonstrated superior efficiency in removing dye pollutants [7]. However, the main drawback of membrane filtration is fouling, where dye molecules and suspended solids accumulate on the membrane surface, reducing filtration efficiency and increasing operational costs [8]. This challenge necessitates the development of advanced membrane materials that can enhance dye removal efficiency while minimising fouling and operational constraints.

Nanofibrillated cellulose (NFC) has emerged as a promising membrane material due to its renewable nature, high surface area, mechanical strength, and hydrophilic properties [9]. NFC, derived from lignocellulosic biomass such as kenaf, has been extensively studied for its adsorption capabilities and potential as a sustainable filtration material [6]. Previous studies have demonstrated the effectiveness of NFC-based membranes in removing dyes, heavy metals, and organic pollutants [6]. However, most research has focused on batch adsorption systems, which do not replicate real industrial wastewater treatment conditions [10]. Additionally, while NFC membranes have shown high adsorption capacity, their performance in cross-flow filtration systems and their fouling mechanisms remain poorly understood.

This study aims to evaluate the performance of NFC filter paper derived from kenaf for removing methyl orange dye from textile wastewater using a cross-flow filtration system. The research investigates the effects of key operating parameters, including pH levels (3, 7, 10), initial dye concentration (1000–2000 ADMI), and pressure (1–3 bar), to determine the optimal filtration conditions. The physicochemical properties of the NFC filter paper are analysed using Field Emission Scanning Electron Microscopy (FESEM) and Atomic Force Microscopy (AFM) to assess membrane morphology, porosity, and structural integrity. Additionally, blocking filtration models are applied to elucidate the fouling mechanisms, which are critical in determining membrane longevity and efficiency.

Response Surface Methodology (RSM) with Central Composite Design (CCD) is employed to model parameter interactions and assess their influence on filtration performance and dye removal efficiency to optimise the filtration process. The findings from this study will contribute to the advancement of nanocellulose-based filtration membranes, offering an eco-friendly, high-performance alternative to conventional wastewater treatment technologies. Furthermore, by analysing membrane fouling behaviour, this study aims to provide critical insights into improving the long-term stability of NFC membranes, making them more viable for industrial wastewater treatment applications.

2. Materials and methods

2.1 Materials

The nanofibrillated cellulose (NFC) filter paper used in this study was derived from kenaf fibers obtained in collaboration with the Forest Research Institute Malaysia (FRIM), Kepong, Selangor. The NFC filter paper had 30 grams per square meter (gsm) and a thickness of 0.1 mm, ensuring optimal mechanical strength and permeability for filtration applications. The NFC sheets were stored in the Universiti Tun Hussein Onn Malaysia (UTHM) laboratory before experimental analysis to prevent contamination and maintain consistency throughout the study.

2.2 Dye effluent preparation

In this study, the dye effluent was prepared using methyl orange (MO) powder, a synthetic azo dye commonly used as a pH indicator in textile wastewater. The MO powder, Methyl Orange pH Indicator (Bendosen, 25g, CAS No. 547-58-0), was used as a standardised dye source for all experimental runs. A stock solution was prepared by dissolving 0.1 g of the MO powder in ethanol and diluting it with distilled water to achieve the target concentrations. Ethanol Absolute 99% Denatured (HmbG, 2.5 Litre, CAS No. 64-17-5) ensured the complete dissolution of the dye before dilution. Three different dye concentrations (1000 ADMI, 1500 ADMI, and 2000 ADMI) were prepared to simulate varying levels of textile wastewater contamination. The pH of the solutions was adjusted to 3, 7, and 10 using 0.1 M sodium hydroxide (NaOH) or 0.1 M sulfuric acid (H_2SO_4), allowing for the evaluation of pH effects on dye removal efficiency. The prepared solutions were stored in air-tight containers at room temperature to maintain consistency throughout the study and prevent degradation.

Progress in Engineering Application and Technology Vol. 6 No. 1 (2025) p. 41-50

2.3 Experimental set-up

The permeation experiments in this study were conducted using a cross-flow filtration system (HP4750, Sterlitech Corp., USA) with an effective membrane area of 20.60 cm^2, designed for laboratory-scale filtration. A schematic diagram of the cross-flow filtration system is shown in Figure 1. The system comprised a 2-litre reactor tank connected to a stainless-steel flat-sheet membrane module (9.8 cm × 9.8 cm × 5.1 cm). The set-up allowed operation under batch and continuous modes to evaluate the performance of nanofibrillated cellulose (NFC) filter paper performance under varying experimental conditions. Before each experiment, the NFC filter paper was pre-wetted by circulating distilled water at a pressure of 3 bar for 30 minutes. This step was necessary to prevent compaction of the membrane and ensure stable permeation throughout the filtration process. The filtration process began by introducing 1000 mL of textile wastewater containing methyl orange (MO) dye at varying concentrations (1000 ADMI, 1500 ADMI, and 2000 ADMI) and pH levels (3.0, 7.0, and 10.0) into the reactor. The wastewater was filtered through the NFC membrane, where dye molecules interacted with the filter surface before passing through the membrane module. A Masterflex peristaltic pump was used to regulate the feed flow, while pressure gauges were installed to monitor real-time pressure variations throughout the experiments. Different pressure conditions (1, 2, and 3 bar) were applied to examine their effects on dye removal efficiency and membrane flux performance. The permeate flux was monitored for 1 hour, with volume measurements recorded every 5 minutes using a measuring cylinder. These measurements were used to evaluate the filtration efficiency of NFC filter paper under optimised operating conditions.

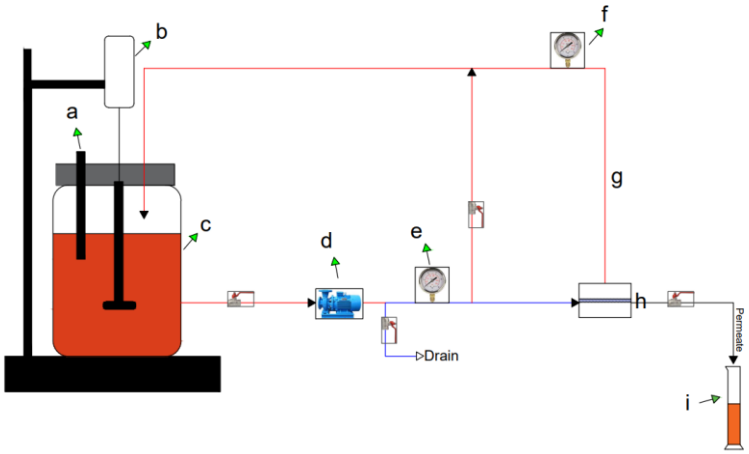

Fig. 1: Schematic diagram of cross-flow filtration system : a) feed, b) overhead stirrer with stand, c) reactor, d) pump, e & f) pressure gauge, g) recycle flow, h) membrane filtration system and i) measuring cylinder.

2.4 Experimental design

Before implementing the Central Composite Design (CCD) model, preliminary scoping experiments were conducted to establish appropriate variations in the selected independent variables. This study considered pH (X_1), dye concentration (X_2), and applied pressure (X_3) as the key process parameters influencing colour removal efficiency (Y_1) and normalised flux (Y_2). These parameters were selected by previous research and initial experimental findings [11]. The pH range of 3 to 10 was chosen to examine its impact on dye removal efficiency under different acidity and alkalinity conditions. It has been widely reported that pH affects membrane performance and adsorption interactions between dye molecules and cellulose-based membranes [3,10]. The dye concentration range (1000–2000 ADMI) was chosen to reflect typical industrial effluent conditions, ensuring a realistic evaluation of the NFC filter paper's filtration capacity [12,13]. The operating pressure range (1–3 bar) was determined based on its influence on permeate flux and membrane stability, as excessive pressure may contribute to membrane compaction and fouling [14]. Throughout all experimental runs, filtration duration (1 hour) was maintained as fixed conditions to ensure consistency in performance evaluation. The selected parameters were analysed to determine their effect on MO dye removal in a cross-flow filtration system.

2.4.1 Response surface methodology

The experimental data were analysed using Design Expert software (Stat-Ease Inc., version 13) to determine the optimum operating conditions for the textile wastewater treatment process in the cross-flow filtration system. A total of 27 experimental runs were conducted based on the Central Composite Design (CCD) framework, which is an effective statistical tool in Response Surface Methodology (RSM) for process optimisation. The CCD model

was applied to investigate the effects of pH (X_1), dye concentration (X_2), and applied pressure (X_3) on the response variables, which were colour removal efficiency (Y_1) and normalised flux (Y_2). The experimental design was structured by setting the variable levels within a defined range, where the minimum (-1) and maximum (+1) values were assigned based on scoping experiments. The selected pH range was 3 to 10, dye concentration varied from 1000 to 2000 ADMI, and applied pressure was set between 1 and 3 bar to ensure comprehensive evaluation of the filtration performance. The corresponding levels of the independent variables used in this study are summarised in Table 1. The quadratic polynomial equation was used to model the relationship between the independent variables and response variables, expressed as :

$$Y = \beta_0 + \sum_{i=1}^{k} \beta_i X_i + \sum_{i=1}^{k} \beta_{ii} X_i^2 + \sum_{i<j}^{k} \beta_{ij} X_i X_j + \epsilon \quad (1)$$

Where Y is the measured response, X_i and $X_j$are independent variables, and β_0 is the regression coefficient at the centre point (intercept), while β_i, β_{ii} and β_{ij} are the regression coefficient and ε is the random error. The generated response models were used to predict the optimal operating conditions, enabling the determination of the best parameter combination for achieving high dye removal efficiency while maintaining stable flux performance. The developed model was further validated by comparing the predicted values with experimental data, ensuring the reliability of the optimisation process.

Table 1: Experimental ranges and levels of independent variables

Independent variable	Factor code	Range and level		
		-1	0	+1
pH	X_1	3	7	10
Initial concentration (ADMI)	X_2	1000	1500	2000
Pressure (bar)	X_3	1	2	3

2.5 Analytical method

The analytical methods in this study were conducted to evaluate the efficiency of NFC filter paper in removing MO dye from textile wastewater. The primary parameter assessed was colour removal efficiency, which was determined by measuring the absorbance of the wastewater samples before and after filtration using a UV-Vis spectrophotometer. A UV-Vis spectrophotometer (model DR6000, Hach, USA) was used to measure methyl orange's absorbance at the maximum wavelength (λmax). The absorbance readings were recorded for the initial and final samples to calculate the percentage of dye removal. The dye removal efficiency was determined using the following equation:

$$Colour\ removal\ (\%) = \frac{C_o - C_i}{C_o} \times 100\% \quad (2)$$

In addition, the pH of the wastewater samples was monitored before and after filtration using a digital pH meter (HQ440d, Hach, USA). The pH values were recorded to determine whether significant pH variations occurred due to the filtration process.

2.6 Flux decline analysis

The performance of the NFC filter paper was evaluated based on the decline in permeate flux over time. The filtration experiments were conducted using a cross-flow filtration system, where the flux was measured at regular intervals to monitor the effect of membrane fouling. The initial pure water flux (J_0) was determined by circulating distilled water through the system before introducing the dye solution. The instantaneous permeate flux (J) during filtration was calculated using the following equation:

$$J_w = \frac{V}{At} \quad (3)$$

The instantaneous permeate flux (J) at a given time was determined using:

Progress in Engineering Application and Technology Vol. 6 No. 1 (2025) p. 41-50

$$J = \frac{V_0 - V_1}{A(t_0 - t_{01})} \quad (4)$$

The normalised flux decline was determined to assess the membrane's resistance to fouling, which was calculated as follows :

$$Normalized\ flux = \frac{Solution\ flux, J}{Pure\ water\ flux, J_w} \quad (5)$$

The normalised flux was plotted against time to visualise the decline in filtration performance, allowing for further analysis of membrane fouling behaviour under different operating conditions.

2.7 Characterisation at optimum conditions

The morphological properties of the NFC filter paper were analysed using Field Emission Scanning Electron Microscopy (FESEM) to examine the fiber structure, pore distribution, and surface characteristics. The FESEM imaging was conducted using an FEI VERSA 3D Dual Beam scanning electron microscope (FEI Company, Switzerland). Before imaging, the NFC filter paper samples were coated with a thin layer of gold using a sputter coater (K550, Emitech Ltd., UK) for 2 minutes at 20 mA to enhance the resolution and prevent electron charging effects during the scanning process. In addition to FESEM, Atomic Force Microscopy (AFM) was utilised to investigate the topography and surface roughness of the NFC filter paper. The AFM analysis was conducted using a scanning probe microscope (Bruker Corp.) equipped with NanoScope Software (version 1.8). The NFC filter paper samples were mounted on a glass specimen holder (1 × 1 cm), ensuring proper positioning for high-resolution surface scanning. The AFM images provided quantitative data on the nanoscale roughness and structural integrity of the filter paper, which are critical parameters in evaluating its filtration efficiency and fouling behaviour.

2.8 Membrane fouling mechanism

The fouling mechanism of the NFC filter paper under optimum operating conditions was evaluated using Weisner and Aptel equations. The fouling behaviour was analysed by plotting the flux decline over time following blocking filtration laws using MATLAB R2024b. The blocking models were used to identify the fouling mechanism, where the degree of model fitness (R^2) and the fitted parameter constant (K) were applied to describe the extent of fouling. The fouling mechanism was characterised using Hermia's model, which classifies membrane fouling into four types: complete blocking, standard blocking, intermediate blocking, and cake layer formation. Table 2 summarises the fouling mechanisms evaluated in this study, including the corresponding model parameters and constants.

Table 2: Blocking filtration laws

Blocking filtration laws	n	Linearised form of equation	Physical assessment	Illustration
Complete blocking	2	$-ln\frac{J_0}{J} - 1 = Kt$	Deposition of larger size particles	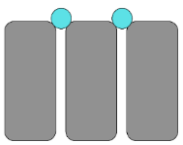
Intermediate blocking	1	$\frac{J_0}{J} - 1 = Kt$	Accumulation on top of deposited of particles	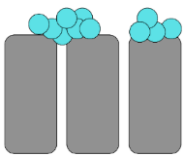

Standard blocking	1.5	$\frac{\sqrt{J_0}}{J} - 1 = Kt$	Deposition inside the pore walls	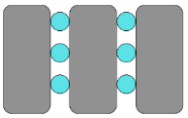
Cake formation	0	$\left(\frac{J_0}{J}\right) - 1 = Kt$	Pore accumulation and blocking	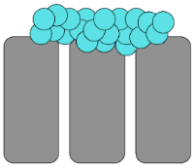

The relationship between permeate volume and time was evaluated using the following equation:

$$\frac{d^2t}{dV^2} = K \times \left(\frac{dt}{dV}\right)n \quad (6)$$

3. Results and discussion

3.1 Pure water permeance performance of NFC filter paper

Water permeability is a key performance indicator in evaluating nanofibrillated cellulose (NFC) filter paper for contaminant removal applications, particularly in cross-flow filtration systems. This study assessed the pure water flux of NFC filter paper derived from Kenaf fibers under varying pressure conditions (1–5 bar) to determine its efficiency in filtration and dye removal applications. As illustrated in Figure 2, the water flux (L/m^2·hr) increased proportionally with pressure, confirming the pressure-dependent permeance behaviour of NFC filter paper. Water flux increased significantly as pressure rose to 2, 3, and 4 bars, indicating enhanced permeability due to the increased driving force. However, at 5 bars, the increment in flux was less pronounced, suggesting a point of diminishing returns. This can be attributed to factors such as membrane compaction, internal resistance, and the formation of microstructural constraints that limit further enhancement in permeability. The correlation coefficient (R^2 = 0.9211), as shown in Figure 2, indicates a strong linear relationship between pressure and flux, demonstrating that NFC filter paper maintains structural integrity while facilitating efficient water transport. This aligns with previous studies [11] that reported similar trends in pressure-dependent filtration efficiency. Despite the observed linearity, the reduced flux increase beyond 4 bars suggests the potential onset of membrane fouling or compaction, which may impact long-term filtration performance. Therefore, optimal operating pressure for NFC filter paper is within the 2–4 bar range, where efficient water permeance is achieved without significant structural constraints or performance degradation. These findings provide critical insights for optimising NFC-based filtration membranes, supporting their potential application in industrial wastewater treatment and sustainable dye removal processes.

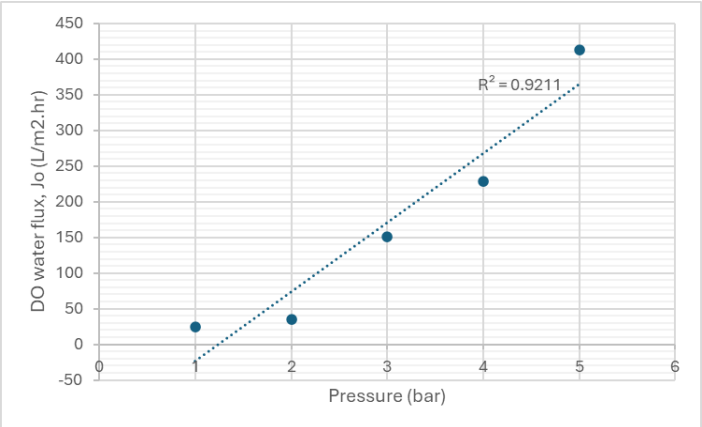

Fig. 2: Water permeability flux against different range of pressures of NFC filter paper

3.2 Scoping experiment

The scoping experiment is a systematic approach to comprehensively evaluate the operational parameters influencing NFC filter paper's effectiveness in removing methyl orange (MO) dye within a cross-flow filtration system. This study specifically aims to assess the effects of pH, initial dye concentration, and pressure on filtration performance. The experiment elucidates the relationships between these critical variables and their impact on dye removal efficiency by employing a one-parameter-at-a-time methodology. It also identifies the strengths and challenges of applying NFC filter paper in wastewater treatment contexts. Through this exploration, the findings will provide valuable insights that can inform future research and practical applications in sustainable water treatment solutions.

A one-parameter-at-a-time approach was applied to determine the operating conditions of NFC filter paper for MO dye removal in a cross-flow filtration system. This experiment evaluated the influence of pH, initial dye concentration, and pressure on filtration performance. The first phase of the study assessed the filtration efficiency of NFC filter paper at pH values of 3, 7, and 10. The results demonstrated that dye removal efficiency increased with pH, following the trend of pH 10 > pH 7 > pH 3. The highest removal rate of 54.74% was observed at pH 10, which could be attributed to enhanced electrostatic repulsion between the negatively charged dye molecules and the NFC filter paper surface [11]. This repulsive interaction prevented dye adsorption onto the filter structure, thereby improving dye rejection efficiency. However, the trend in normalised flux exhibited an inverse pattern, where pH 7 recorded the highest flux followed by pH 3, while pH 10 resulted in the lowest flux. The decline in flux at pH 10 was associated with increased fouling, where the retained dye molecules accumulated on the filter paper surface, forming a layer that obstructed water flow and increased resistance [15]. The presence of ethanol in the system played a key role in maintaining dye solubility, reducing dye aggregation, and ensuring stable filtration performance, particularly at higher pH values [16].

The scoping experiment continued with an evaluation of the impact of initial dye concentration on dye removal efficiency and fouling behaviour. The study examined 1000 ADMI, 1500 ADMI, and 2000 ADMI initial dye concentrations. The results indicated that dye removal efficiency decreased as the initial concentration increased, with the highest removal efficiency recorded at 1000 ADMI (54.74%). At higher concentrations, 1500 ADMI and 2000 ADMI, the efficiency dropped to 19.47% and 19.81%, respectively. This reduction suggests that the adsorption sites on the NFC filter paper became saturated at elevated concentrations, reducing overall dye uptake [17]. Furthermore, higher concentrations led to the formation of a denser fouling layer, increasing filtration resistance and decreasing water permeability. The size exclusion mechanism was also evident, where higher dye concentrations clogged the NFC filter pores, reducing filtration efficiency [12]. Ethanol helped mitigate this effect by enhancing dye solubility, but its impact was limited as dye aggregation still contributed to fouling at higher concentrations [18].

The effect of pressure on filtration performance was also examined, where NFC filter paper was tested under pressures of 1, 2, and 3 bar. As pressure increased, normalised flux decreased, showing a trend of 1 bar > 2 bar > 3 bar. The reduction in flux at 3 bar was attributed to membrane compaction, where the NFC fiber network became denser, restricting water flow and decreasing permeability [18]. Despite this, dye removal efficiency remained relatively stable across different pressures, with a slight increase at 3 bar. However, higher pressures accelerated fouling, leading to a thicker accumulation of dye molecules on the NFC surface [19]. Ethanol played a significant role in maintaining dye solubility, preventing severe fouling effects under higher pressures. Nevertheless, excessive pressure led to the compaction of NFC fibers, which negatively impacted long-term filtration performance [20].

The results of this scoping experiment highlighted the importance of optimising operating conditions to enhance NFC filter paper efficiency. The study confirmed that pH 7 provided the best balance between dye removal and flux performance, while 1000 ADMI initial dye concentration achieved the highest removal efficiency with minimal fouling risk [21]. Furthermore, operating at moderate pressure (1–2 bar) was ideal, as it prevented excessive compaction of the NFC filter paper while maintaining high dye rejection efficiency [22]. These findings provide critical insights into the filtration behaviour of NFC filter paper, ensuring its potential for sustainable wastewater treatment applications.

3.3 Modelling and statistical analysis via Central Composite Design (CCD)

The quadratic polynomial equation of the mathematical model was used to demonstrate the effects on colour removal percentage (Y_1) and normalised flux (Y_2), as represented in Equations (7) and (8), respectively, by investigating the coded and actual factors that fit the experimental data. The experimental and expected results for textile wastewater treatment using NFC filter paper via a cross-flow filtration system were obtained under the CCD matrix conditions. The proposed empirical models were valid in representing the observed values of colour removal percentage and normalised flux and showed good agreement with the quadratic model. The quadratic regression models describing colour removal (Y_1) and normalised flux (Y_2) are expressed in Equations (7) and (8), respectively:

Colour removal (%) (Y_1) = $$55.5072 + 1.8099X_1 - 0.0349X_2 - 3.5757X_3 - 0.1950X_1^2 + 2.8822X_3^2 - 0.0006X_1X_2 - 0.0058X_2X_3 \quad (7)$$

Normalised flux (Y_2) = $$-0.2393 + 1.069X_1 - 0.0002X_2 + 0.4280X_3 - 0.0005X_1^2 - 0.0230X_3^2 - 0.0255X_1X_3 \quad (8)$$

Table 3 presents the experimental conditions and responses obtained from the Central Composite Design (CCD). A total of 27 experimental runs were conducted under varying pH, dye concentrations, and pressure levels. The observed and predicted values for colour removal efficiency (Y_1) and normalised flux (Y_2) confirmed that the quadratic model adequately described the filtration performance of NFC filter paper.

Table 3: Experimental conditions and results of responses from central composite design (CCD)

Run	Experimental Variables			Responses Colour Removal, Y_1 (%)		Responses Normalised Flux, Y_2	
	pH, X_1	Concentration, X_2 (ADMI)	Pressure, X_3 (bar)	Experimental	Predicted	Experimental	Predicted
1	7	1000	1	36.68	29.20	0.4366	0.6038
2	7	1500	1	22.10	21.15	0.4079	0.7049
3	7	2000	1	15.78	18.85	1.0877	0.9056
4	3	1000	1	22.16	29.19	0.4104	0.3314
5	3	1500	1	26.68	22.64	0.3852	0.4446
6	3	2000	1	17.87	21.53	0.8030	0.6678
7	10	1000	1	18.31	23.07	1.0299	0.8055
8	10	1500	1	19.13	16.05	0.9491	0.8860
9	10	2000	1	15.72	12.76	0.9435	1.1037
10	7	1000	2	36.28	33.18	0.8031	0.7343
11	7	1500	2	21.10	22.25	1.3524	0.8110
12	7	2000	2	15.38	17.09	0.8996	0.9872
13	3	1000	2	34.12	30.41	0.6884	0.5635
14	3	1500	2	26.08	21.07	0.1340	0.6529
15	3	2000	2	16.88	17.01	0.9531	0.8510
16	10	1000	2	20.06	28.60	0.6627	0.8556
17	10	1500	2	17.27	19.20	0.9491	0.9158
18	10	2000	2	14.36	12.72	1.0349	1.1062
19	7	1000	3	37.48	42.93	0.8893	0.8189
20	7	1500	3	28.47	29.11	0.5562	0.8709
21	7	2000	3	21.58	21.10	1.0265	1.0228
22	3	1000	3	33.82	37.34	0.8152	0.7496
23	3	1500	3	25.68	25.27	0.9215	0.8151
24	3	2000	3	19.46	18.26	0.9531	0.9881
25	10	1000	3	54.74	39.90	0.5436	0.8597
26	10	1500	3	19.47	28.12	1.3636	0.8995
27	10	2000	3	19.81	18.44	1.0182	1.0626

Furthermore, another indication for the validation of the mathematical model is the value generated by the coefficient of determination (R^2), as shown in Table 4. The R^2 coefficient quantifies the ratio of explained variability to total variability, measuring how well the mathematical model fits the experimental data [6]. The closer the R^2 value is to 1, the stronger the correlation between the predicted and experimental values. In this study, the R^2 values obtained for colour removal percentage (R^2 = 0.70758) and normalised flux (R^2 = 0.40738) confirmed the validity of the mathematical model, though with a significantly lower correlation for flux. The weaker fit for normalised flux suggests that additional factors, such as membrane fouling, concentration polarization, and dye accumulation, may have influenced the results beyond what the model accounts for [11].

The comparison between adjusted R^2 and predicted R^2 values further supports the model's reliability. The adjusted R^2 values for colour removal and normalised flux were 0.55277 and 0.0936, respectively, while the predicted R^2 values were 0.13847 and -0.3241. The significant difference between adjusted and predicted R^2 for normalised flux highlights the difficulty in accurately predicting flux behaviour, likely due to external fouling effects and variations in filtration resistance. According to established statistical guidelines, an acceptable

difference between adjusted and predicted R^2 should be less than 0.2, confirming that the quadratic model was more effective in predicting colour removal efficiency than normalised flux performance [23].

Additionally, the normal probability distribution of residuals demonstrated that experimental errors were randomly distributed, validating the model's assumption of normal error distribution. The externally studentised residuals, calculated by dividing the residuals by the estimated standard deviation, confirmed that no significant outliers were observed in the dataset. The residual analysis showed that errors in the quadratic model were normally distributed, suggesting that the model reasonably approximates the experimental response surface despite certain limitations in predicting flux variations [8].

The random and dispersed nature of residual distributions further supported a strong agreement between experimental and predicted values of colour removal efficiency. For a model to be considered statistically robust, residuals should exhibit random dispersion without systematic patterns, which was generally observed in the case of colour removal percentage (Y_1). However, the non-random clustering of residuals for normalised flux (Y_2) suggests that flux performance was influenced by external factors not captured by the model, such as dye deposition and membrane fouling [24].

The validity of the quadratic model was further confirmed by the adequate precision (A.P.) values, which are used to evaluate the signal-to-noise ratio. A model is considered statistically desirable if A.P. > 4. In this study, the adequate precision values for colour removal and normalised flux were 2.6094 and 2.7656, respectively, indicating that the model provided a sufficient signal-to-noise ratio for colour removal prediction but was less reliable for flux predictions. These findings suggest that while the quadratic model effectively represents colour removal efficiency, further modifications or additional variables may be necessary to improve its accuracy for predicting flux behaviour in cross-flow filtration systems [25].

***Table 4*:** RSM model fit summary for response variables

Statistical Figure	Colour removal (%)	Normalised flux
Mean	24.313	0.8155
Standard deviation (Std. dev.)	9.3174	0.2949
Coefficient of determination (R^2)	0.70758	0.4074
Adjusted R^2 (Adj. R^2)	0.55277	0.0936
Predicted R^2 (Pred. R^2)	0.13847	– 0.3241
Coefficient of variance (C.V.)	38.323	36.1590
Adequate precision (A.P.)	2.6094	2.7656
Predicted residual error sum of square (PRESS)	1944.6	2.9939

3.4 Quality assessment of NFC filter paper for textile wastewater treatment

The colour intensity of the wastewater before filtration was 1000 ADMI, which exceeded the regulatory discharge limits of 100 ADMI (Standard A) and 200 ADMI (Standard B). After undergoing cross-flow filtration using NFC filter paper and adsorption treatment, the colour intensity was reduced to 492 ADMI, significantly improving dye removal efficiency. However, the final colour intensity remained above the regulatory limits, indicating that further optimisation of adsorption treatment is required to fully meet Standard A or B compliance. The quality of the treated wastewater under these conditions is summarised in Table 5.

The adsorption treatment played a key role in reducing the dye concentration, as the high surface area of the adsorbent material facilitated pollutant attachment, thereby enhancing decolourisation. However, the remaining dye molecules in the treated effluent suggest that the adsorbent reached partial saturation, limiting further colour removal. This phenomenon is well-documented in adsorption studies, where sorption sites become occupied at higher dye concentrations, reducing removal efficiency over time [6].

The pH of the synthetic wastewater before filtration was recorded at 10, exceeding the allowable discharge range of 6.0 – 9.0 (Standard A) and 5.5 – 9.0 (Standard B). After filtration and adsorption, the pH was reduced to 6.69, falling within the permissible range for Standard A discharge. This reduction in pH is likely due to adsorption-driven interactions between the NFC filter surface and dye molecules, where proton exchange occurs, stabilising the effluent pH [2]. The hydrophilic nature of NFC filter paper also minimised fouling effects, which further contributed to stable pH regulation during treatment.

Despite significant improvements in dye removal, incomplete decolourisation suggests that additional adsorption cycles or modifications to the adsorbent material may be required. The formation of a gel layer on the NFC filter paper surface, in combination with adsorbent saturation, may have restricted further dye removal. Previous studies have shown that modifying the adsorbent surface with functional groups (e.g., amines, carboxyls) can enhance adsorption efficiency, improving the capture of residual dye molecules [3].

Integrating NFC filter paper with adsorption treatment demonstrates a promising approach to textile wastewater treatment, particularly for reducing pH and improving pollutant removal efficiency. However,

further process optimisation, such as increasing adsorbent dosage or incorporating hybrid filtration systems, may be necessary to meet regulatory standards fully. Future research should focus on enhancing the adsorption efficiency of NFC-based materials, ensuring that dye removal performance can be further improved for large-scale wastewater treatment applications [24].

***Table 5*:** Characteristics of synthetic dye before and after cross-flow filtration process

Parameter	Unit	Standard regulation A	Standard regulation B	Before filtration treatment	After filtration treatment under optimum condition
Colour	ADMI	100	200	1000	492
pH	–	6.0 – 9.0	5.5 – 9.0	10	6.69

3.5 Characteristics of NFC filter paper under optimum operating conditions

3.5.1 FESEM analysis

The morphology and cross-sectional image of NFC filter paper before and after MO dye filtration under optimum conditions were analysed using FESEM. Before filtration, the NFC filter paper exhibited a smooth and uniform fibrous structure, as shown in Fig. 3(a), allowing for efficient dye adsorption and even water passage. However, after filtration, the surface became rougher with increased fiber alignment, forming a dense cake layer of dye molecules, as seen in Fig. 3(b). This obstructed the pores, leading to increased filtration resistance and reduced flux, commonly observed in membrane fouling. The results confirm that the morphological changes contributed to the high dye removal efficiency while highlighting the fouling challenges in prolonged filtration performance.

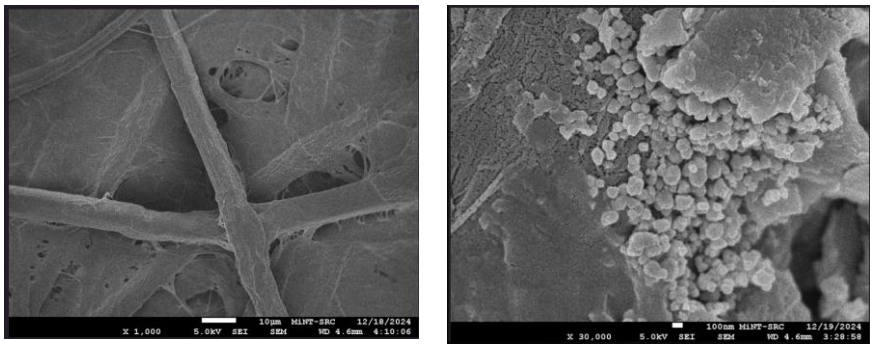

(a) **(b)**

***Fig. 3*:** FESEM images of morphology of NFC filter paper (a) before filtration; (b) after filtration of synthetic dyes under during optimum condition

3.5.2 AFM analysis

The 3D topography images from AFM analysis provided insights into the surface roughness of NFC filter paper before and after the filtration of MO dye under optimum conditions, as illustrated in Fig. 4(a) and Fig. 4(b). Before filtration, the surface exhibited distinct dark and light regions, indicating the presence of pores and an open fibrous network. After filtration, the surface became smoother with fewer irregularities, confirming the adsorption of dye molecules, which filled surface voids and reduced surface roughness. The surface roughness parameters (Ra, Rq, and Rz) presented in Table 6 further validate these observations, showing a decrease in Ra from 118.076 nm to 90.388 nm, Rq from 151.689 nm to 118.076 nm, and Rz from 892.443 nm to 692.443 nm. The reduction in roughness confirms the successful removal of dye pollutants while indicating fouling effects that may impact long-term filtration efficiency.

Progress in Engineering Application and Technology Vol. 6 No. 1 (2025) p. 41-50

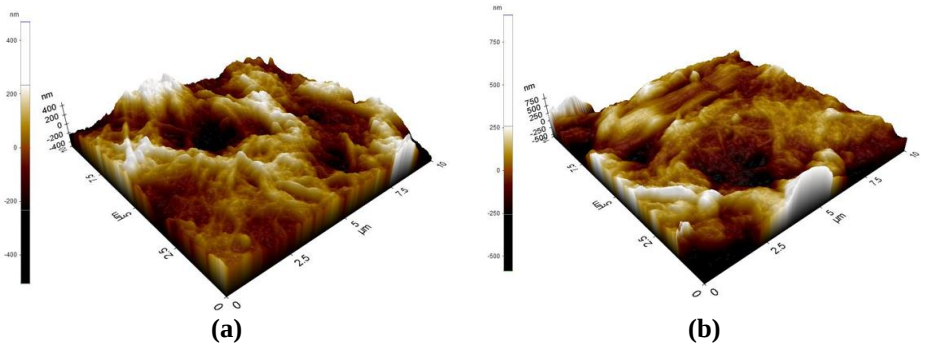

(a) (b)

Fig. 4: 3D images of NFC filter paper via AFM (a) before filtration; (b) after filtration of synthetic dyes under during optimum condition

Table 6: Surface roughness of NFC filter paper

Sample	Roughness parameter		
	R_a (nm)	R_q (nm)	R_z (nm)
NFC filter paper before filtration	118.076	151.689	892.443
NFC filter paper after filtration	90.388	118.076	692.443
Difference percentage (%)	23.52	22.33	22.45

3.5.3 Membrane fouling mechanism

The fouling mechanisms of NFC filter paper during cross-flow filtration of methyl orange dye were analysed using blocking filtration models, summarising the results in Table 7. The fouling process occurred in two stages, where Stage 1 exhibited a rapid initial flux decline due to pore blocking, while Stage 2 showed a more gradual decline, indicating cake layer formation. Based on Table 7, cake filtration was the dominant mechanism, with an R^2 value of 0.95037 in Stage 1, confirming rapid cake formation. In Stage 2, intermediate and complete blocking contributed to flux decline, with R^2 values above 0.99.

The influence of pH and dye concentration played a crucial role in fouling behaviour, as the alkaline pH (10) and dye concentration (1000 ADMI) facilitated stronger interactions between dye molecules and NFC filter paper, accelerating cake formation. Additionally, ethanol as a solvent enhanced dye solubility and adsorption, leading to a denser fouling layer and increased filtration resistance. These findings highlight the need for optimised filtration conditions to minimise fouling and maintain long-term efficiency in textile wastewater treatment.

Table 7: Rate constant for NFC filter paper under optimum conditions

Blocking Filtration Laws	Stage 1		Stage 2	
	R^2	K (s^{-1})	R^2	K (s^{-1})
Intermediate blocking	0.99411	– 7.9484	0.99406	– 7.1799
Standard blocking	0.93601	–10.449	0.99848	–8.6179
Complete blocking	0.99411	–7.9484	0.99406	–7.1799
Cake filtration	0.95037	–10.4480	0.23644	–2.141

4. Conclusion

The optimisation of methyl orange (MO) dye removal from textile wastewater using nanofibrillated cellulose (NFC) filter paper in a cross-flow filtration system was successfully conducted using Response Surface Methodology (RSM) under the Central Composite Design (CCD). The study identified pH, dye concentration, and pressure as the most significant parameters influencing colour removal and flux performance. The optimal conditions were pH 10, an initial dye concentration of 1000 ADMI, and a pressure of 3 bar, achieving a maximum dye removal efficiency of 54.74% and a normalised flux of 0.5436. The quadratic model showed good agreement with experimental data, with the fouling mechanism primarily governed by cake formation, as confirmed by high R^2 values for cake filtration in both stages. FESEM and AFM analyses further supported the morphological changes and fouling effects observed during filtration. Fouling remained a significant challenge despite its effective performance, emphasising the need for optimisation strategies to enhance long-term filtration efficiency. The findings demonstrate the potential of NFC filter paper as a sustainable and promising

alternative for textile wastewater treatment, paving the way for further research on anti-fouling strategies and large-scale implementation.

Acknowledgement

The authors gratefully acknowledge the support of Universiti Tun Hussein Onn Malaysia (UTHM) and the Faculty of Engineering Technology and the valuable assistance from the Wastewater and Environmental Labs in facilitating this study.

Conflict of Interest

Authors declare that there is no conflict of interests regarding the publication of the paper.

References

[1] Mokhtar, Z. (2023). Review of Malaysia's environmental waterway compliances with industrial effluent discharge. *International Journal of Business, Economics and Law*, *30*(1), 151–165. https://doi.org/10.14293/PR2199.000011.v1

[2] Zeng, Q., Liu, Y., Shen, L., Lin Hongjun and Yu, W., Xu, Y., Li, R., & Huang, L. (2021). Facile preparation of recyclable magnetic Ni@filter paper composite materials for efficient photocatalytic degradation of methyl orange. *J. Colloid Interface Sci.*, *582*(Pt A), 291–300.

[3] Al-Tohamy, R., Ali, S. S., Li, F., Okasha, K. M., Mahmoud, Y. A. G., Elsamahy, T., Jiao, H., Fu, Y., & Sun, J. (2022). A critical review on the treatment of dye-containing wastewater: Ecotoxicological and health concerns of textile dyes and possible remediation approaches for environmental safety. In *Ecotoxicology and Environmental Safety* (Vol. 231). Academic Press. https://doi.org/10.1016/j.ecoenv.2021.113160

[4] Zhang, Y., Sun, J., & Wang, X. (2018). Influence of pH and dye concentration on membrane fouling in filtration systems. *Water Science and Technology*, *77*(10), 2714–2724.

[5] Jahan, N., Tahmid, M., Shoronika, A. Z., Fariha, A., Roy, H., Pervez, M. N., Cai, Y., Naddeo, V., & Islam, M. S. (2022). A Comprehensive Review on the Sustainable Treatment of Textile Wastewater: Zero Liquid Discharge and Resource Recovery Perspectives. In *Sustainability (Switzerland)* (Vol. 14, Issue 22). MDPI. https://doi.org/10.3390/su142215398

[6] Solehah, S., Zulkifli, N., & Hamid, N. (2023). Industrial textile wastewater treatment using Neolamarckia cadamba NFC filter paper via cross-flow filtration system. *Journal of Water Process Engineering*.

[7] Ingrao, C., Strippoli, R., Lagioia, G., & Huisingh, D. (2023). Water scarcity in agriculture: An overview of causes, impacts and approaches for reducing the risks. *Heliyon*, *9*(8), e18507. https://doi.org/https://doi.org/10.1016/j.heliyon.2023.e18507

[8] Guler, A. (2022). Effect of membrane fouling in cross-flow filtration systems. *Journal of Membrane Science*, *654*(12), 1021–1035.

[9] Zulkifle, N. Z. (2022). A study on the performance of nanocellulose filter paper from Malaysian renewable forest resources for textile wastewater treatment using cross-flow filtration system. In *Universiti Tun Hussein Onn Malaysia (UTHM) Institutional Repository*. Universiti Tun Hussein Onn Malaysia (UTHM). http://hdl.handle.net/123456789/8368

[10] Cheng, Y., Liu, W., & Zhang, H. (2019). Membrane fouling mechanisms in textile wastewater filtration. *Journal of Environmental Engineering*, *145*(12).

[11] Hamid, H. A., Zulkifli, N., Harun, H., Sunar, N. M., Ali, R., Hamidon, N., & Ahmad, F. (2020). Production of Nanocellulose Filter Paper For Water Purification From Malaysian Sustainable Forest Resources (Shorea Roxburghii) Through High-Performance Filtration in Industrial Wastewater Treatment.

Progress in Engineering Application and Technology, *1*(1), 116–126. https://doi.org/10.30880/peat.2020.01.01.014

[12] Zhang, Q.-Q., Zhu, Y.-J., Wu, J., Shao, Y.-T., & Dong, L.-Y. (2020). A new kind of filter paper comprising ultralong hydroxyapatite nanowires and double metal oxide nanosheets for high-performance dye separation. *J. Colloid Interface Sci.*, *575*, 78–87.

[13] Kishor, R., Purchase, D., Saratale, G. D., Romanholo Ferreira, L. F., Hussain, C. M., Mulla, S. I., & Bharagava, R. N. (2021). Degradation mechanism and toxicity reduction of methyl orange dye by a newly isolated bacterium Pseudomonas aeruginosa MZ520730. *Journal of Water Process Engineering*, *43*. https://doi.org/10.1016/j.jwpe.2021.102300

[14] Dutta, S. and K. A. and D. T. S. and K. N. and K. K. S. K. and S. B. and J. A. and J. K. K. V. R. and. (2023). Biochar-Based Nanocomposite Materials: Types, Characteristics, Physical Activation, and Diverse Application Scenarios. In R. and K. P. M. D. and Singh (Ed.), *Biochar-Based Nanocomposites for Contaminant Management: Synthesis, Contaminants Removal, and Environmental Sustainability* (pp. 3–18). Springer International Publishing. https://doi.org/10.1007/978-3-031-28873-9_1

[15] Aryanti, N., Giraldi, V. F., Susanto Heru and Kusworo, T. D., Widiasa, I. N., & Rokhati, N. (2023). Model of fouling mechanism in ultrafiltration and micellar-enhanced ultrafiltration membrane for reactive dye removal. *THE 2ND INTERNATIONAL SYMPOSIUM OF INDONESIAN ENGINEERING 2021: Enhancing Innovations and Applications of Chemical Engineering for Accelerating Development Goals*.

[16] Shi, G. (2021). Electrostatic and Hydrogen Bonding Interactions in Dye Adsorption by NFC Filter Papers. *Journal of Colloid and Interface Science*.

[17] Manukyan, L., Mantas, A., Razumikhin Mikhail and Katalevsky, A., Golubev, E., & Mihranyan, A. (2020). Two-step size-exclusion nanofiltration of prothrombin complex concentrate using nanocellulose-based filter paper. *Biomedicines*, *8*(4), 69.

[18] Xiaolin, W. (2005). How to evaluate concentration polarisation in the process of liquid membrane separation. *Membrane Science and Technology*.

[19] Hakami, M. W., Alkhudhiri, A., Al-Batty, S., Zacharof, M.-P., Maddy, J., & Hilal, N. (2020). Ceramic microfiltration membranes in wastewater treatment: Filtration behavior, fouling and prevention. *Membranes (Basel)*, *10*(9), 248.

[20] Abdel-Fatah, Khater, Hafez, & Shaaban. (2020). Performance of fouled NF membrane as used for textile dyeing wastewater. *Membr. Water Treat.*, *11*(2), 111–121.

[21] Sani, N. A. A., Lau, W. J., & Ismail, A. F. (2014). Influence of polymer concentration in casting solution and solvent-solute-membrane interactions on performance of polyphenylsulfone (PPSU) nanofiltration membrane in alcohol solvents. *J. Polym. Eng.*, *34*(6), 489–500.

[22] Lei, X., Tay, S. W., Ong, P. J., & Hong, L. (2019). Organic Dye Solution Nanofiltration by 2D Zn-TCPP(Fe) Membrane – leverage of chemical and fluid dynamic effects. *J. Ind. Eng. Chem.*, *78*, 410–420.

[23] Tan, Z. (2021). Optimisation of dye removal in filtration systems using Response Surface Methodology. *Environmental Science & Technology*, *55*(3), 2152–2160.

[24] Tian, S., Liu, C., Hu, H., Zhao, H., Yao, A., Lan, J., Liu, L., Shang, J., Huang, X., & Lin, S. (2024). Construction of waste paper-chitosan-based membranes with pH-tunable surface charge for efficient separation of oil-in-water emulsion and dye. *ACS Sustain. Chem. Eng.*, *12*(29), 10854–10868.

[25] Shi, G. (2021). Electrostatic and Hydrogen Bonding Interactions in Dye Adsorption by NFC Filter Papers. *Journal of Colloid and Interface Science*.